

## Invited Feature Article

## Application of time-resolved circular dichroism to the study of conformational changes in photochemical and photobiological processes

François Hache\*

Laboratoire d'Optique et Biosciences, Ecole Polytechnique, CNRS, INSERM, 91128 Palaiseau, France

## ARTICLE INFO

## Article history:

Received 30 January 2009

Received in revised form 11 March 2009

Accepted 12 March 2009

Available online 25 March 2009

## Keywords:

Time-resolved circular dichroism

Conformational changes

Myoglobin

## ABSTRACT

Circular dichroism is known to be a very sensitive probe of the molecular conformation and implementation of this technique in a pump-probe experiment is very appealing to access information on the dynamics of conformational changes occurring in photochemical or photobiological processes. In the past years, we have developed such techniques in various ways and applied them to several chemical or biological studies which are presented in this article. Applications concern spectroscopic studies of the excited state in ruthenium tris(bipyridyl) or tris(phenanthroline), dynamics of conformational changes in photoexcited binaphthol and study of the conformational changes occurring in photolyzed carboxy-myoglobin. Extension of these techniques towards biological issues such as protein folding is discussed.

© 2009 Elsevier B.V. All rights reserved.

### 1. Introduction

Circular dichroism (CD), the difference in absorption for a left or a right circularly polarized light, is with optical rotation a unique optical characteristics of chiral molecules. Because chirality is primarily a geometrical property, CD is in turn very sensitive to the conformation of molecules. This feature makes CD an attractive probe for stereochemistry and especially for the study of biomolecules [1]. However, development of CD in time-resolved experiments allowing ultrafast conformational changes to be monitored, although a very appealing idea, has not been extensively studied. Seminal work in this direction has been performed by Kliger's group [2] who demonstrated nanosecond-resolved CD in carboxy-myoglobin. Later on, this technology was extended to picosecond time resolution [3]. Since that time, Kliger has pursued this work and developed alternative techniques on time-resolved optical rotation or magnetic CD which he has applied to many biological issues [4].

The major reason for the rareness of such studies despite their recognized potential applications is clearly an experimental issue. Indeed, CD is a rather weak effect and unfortunately, implementation of CD in a time-resolved experiment has proved to give birth to many artefacts which are tremendously difficult to overcome. Our expertise in ultrafast optics and our interest in physical chemistry as well as in fundamental biological processes have pushed us to re-investigate this issue and to develop new schemes of time-resolved

CD (TRCD). Several technical improvements have been brought in order to make these experiments more tractable. In particular, we have come up with a new measurement technique which allows us to eliminate most of the artefacts and to obtain nice results in a user-friendly manner. These technical improvements will be rapidly summarized in Section 2. This new TRCD experiment has been utilized to investigate several issues in chemical or biological molecules which will be described in the following of this paper. In Section 3, spectroscopic studies aiming at measuring the CD spectra of electronically excited states in a ruthenium complex will be presented. In Section 4, we show how TRCD has allowed us to investigate conformational dynamics in excited binaphthol. The dynamics of the dihedral angle is measured and the effects of solvent viscosity or proticity are studied. Investigation of ultrafast conformational changes is indeed one of the most promising applications of TRCD and we have applied this technique to the study of conformational changes following the photodissociation of carboxy-myoglobin. Experiments in the visible and in the UV together with model calculations aiding for the interpretation of results are described in Section 5. Finally, Section 6 is devoted to discussion of the potential extension of this technique towards study of the protein folding problem, one major issue in modern biophysics.

### 2. Materials and methods

#### 2.1. Pump-probe experiment

In order to achieve ultrafast measurements, pump-probe experiments have been utilized for a long time and TRCD experiments are based on the same principle. A first intense light pulse (the

\* Tel.: +33 169335039.

E-mail address: [francois.hache@polytechnique.edu](mailto:francois.hache@polytechnique.edu).

“pump”) is sent onto the sample so as to provoke a change in the molecules which is monitored by a second, weak, delayed pulse (the “probe”). In our experiments, the pump induces a change in the electronic configuration of the studied compounds whereas the probe measures the CD of the excited species. Two cases are then possible. In the first case, the probe is used to investigate the CD of the electronically excited state and information is obtained from the wavelength-dependence of this CD signal. In the second one, a consequence of the electronic excitation is a change in the molecule conformation which is monitored by the probe.

Our experimental set-up is based on a 1 kHz, 150 fs Titanium-Sapphire laser (Spectra-Physics). The pump pulses are most often obtained by frequency-doubling (400 nm) or tripling (267 nm) the output of the laser. On the other hand, extensive use of nonlinear optics for the generation of new frequencies in frequency-mixing stages or in optical parametric amplifiers allows us to have a very versatile source for the probe [5]. Depending on the experiments, we use probe pulses tunable in the visible (400–500 nm) or in the UV (230–350 nm). Pump and probe pulses are focussed on the sample. The delay between the pump and the probe is computer-controlled and can be varied up to 1.5 ns. The sample consists in a fused-silica, 1 mm thick cuvette. A circular translation motion is imposed to the sample in order to avoid cumulative heating effects. For all the experiments, the sample concentration is chosen so that the optical density at the pump wavelength is of the order of unity. It corresponds to concentration in the range 100–300  $\mu\text{M}$ . In every case, the pump energy was kept between 200 and 500 nJ in order not to damage the samples.

## 2.2. TRCD: probe polarization modulation

The most straightforward idea to measure CD with the probe is to modulate its polarization from left to right circular and to measure the subsequent modulation of the transmission of the sample. This idea is close to the one developed by Kliger [2]. In order to achieve probe polarization modulation under the constraint of the 1 kHz rep rate of the laser, we have used a longitudinal Pockels cell. By applying alternately positive and negative high voltage on the Pockels cell ( $\pm 1.5$  kV for 400 nm), one obtains alternately left and right circular polarizations. Detecting the transmitted probe intensity with a photomultiplier tube and de-modulating the signal with a lock-in amplifier locked on the Pockels cell voltage modulation, one readily gets the transmission and the CD of the sample. However, this technique is impaired by the necessity to obtain perfectly symmetrical circular polarizations to avoid artefacts. In order to achieve such a perfect symmetry, we have come up with a stringent alignment procedure of the Pockels cell. Interested readers can find details in Ref. [6]. CD measurements are performed as a function of the pump-probe delays. Due to the weakness of the pump-induced CD changes, strong averaging of the experimental curves was necessary in order to obtain exploitable data. This technique was successfully implemented in the visible for the study of ruthenium complexes and myoglobin. One advantage of this technique is that it allows steady-state CD measurement to be performed as well as TRCD ones.

## 2.3. TRCD: use of a Babinet–Soleil compensator

The above-described technique, although straightforward, is unfortunately not easy to use because long-time averaging is often not compatible with Pockels cell drifts. For this reason, we have re-investigated the problem of detecting pump-induced CD and proposed a quite new scheme based on the measurement of the probe ellipticity. Indeed, it is well known that when a linearly polarized beam passes through a chiral sample, its polarization becomes elliptical. The idea is therefore to measure the change in the probe

beam ellipticity induced by the pump. In this new scheme, we do not modulate the polarization of the probe but keep the probe linearly polarized. This feature presents the tremendous advantage that it removes the artefacts which induced so dramatic problems in the previous technique. In order to measure the probe ellipticity, we put the sample between a polarizer and a crossed analyzer and insert a Babinet–Soleil compensator. A Babinet–Soleil compensator can be seen as a waveplate for which one can finely tune the retardation. Measuring the transmitted intensity for small Babinet–Soleil retardations allows a straightforward determination of the beam ellipticity. As such, this set-up is not very efficient to measure the CD because of the smallness of the signal. However, things are completely different when one wants to access the pump-induced CD. To do so, we insert a mechanical chopper on the pump path and measure the transmitted probe intensity with a photomultiplier tube (hereafter called the “PM” signal) and its modulated part with a lock-in amplifier (hereafter called the “LI” signal) as a function of the Babinet–Soleil retardation. Calling  $\varphi$  the Babinet–Soleil retardation, very simple algebra, detailed in Ref. [7] yields for the two measured signals:

$$PM = \varphi^2 + C_1 \quad \text{and} \quad LI = -\delta\alpha L \varphi^2 + \frac{\delta CD}{2} \varphi + C_2.$$

In these equations,  $C_1$  and  $C_2$  are constants,  $\delta\alpha L$  is the pump-induced absorption change and  $\delta CD$  the pump-induced CD change. Examination of the formulas shows that comparing the curvature of the  $PM$  and  $LI$  parabolas directly yields  $\delta\alpha L$  and that the  $LI$  parabola is shifted compared to the  $PM$  one by  $\delta CD/4\delta\alpha L$ . This shift is easily measurable (especially when  $\delta\alpha L$  is not too strong) and this technique allows  $\delta\alpha L$  and  $\delta CD$  to be detected in the  $10^{-4}$  range. The measurements therefore consist in recording the two parabolas for a fixed pump-probe delay and to extract change in absorption and in CD by fitting them. Examples of the measured parabolas are given in the inset of Fig. 6.

This new technique presents several advantages. As already stated, it is free from most of the artefacts since there is no longer modulated circular polarizations for the probe, which represents a remarkable improvement. Use of a mechanical chopper on the pump further increases the signal-to-noise ratio and allows weak signals to be detected with much less averaging than with the other technique. The major drawback of this technique is that it is efficient for the measure of the pump-induced CD on the condition that the change of absorption is not too strong. Fortunately, it is often the case, especially in the UV.

This technique has been used for measurements in binaphthol and in myoglobin in the UV range. As will be discussed in the last section, it should be possible to extend it to many experimental configurations.

## 3. Excited-state CD spectra in ruthenium complexes

Ruthenium complexes such as ruthenium(II) tris(bipyridyl) and ruthenium(II) tris(phenanthroline) have been extensively studied due to their remarkable properties leading to applications in energy and electron-transfer processes, chemi- and electrochemiluminescent processes and supramolecular assemblies [8]. They are also known to be efficient DNA intercalation compounds [9]. Most of these applications rely on the metal-to-ligand charge transfer (MLCT) band which lies in the visible: Upon photon absorption, an electron is transferred from the metal towards the ligands. Consensus now exists that the electron is very rapidly localized on a unique ligand in ruthenium(II) tris(bipyridyl) [10]. Identical conclusion holds for ruthenium(II) tris(phenanthroline) [11].

The three ligands assume a propeller shape making these complexes chiral with two stable enantiomeric forms  $\Lambda$  and  $\Delta$ . Enantiomerically pure samples exhibit a CD spectrum charac-

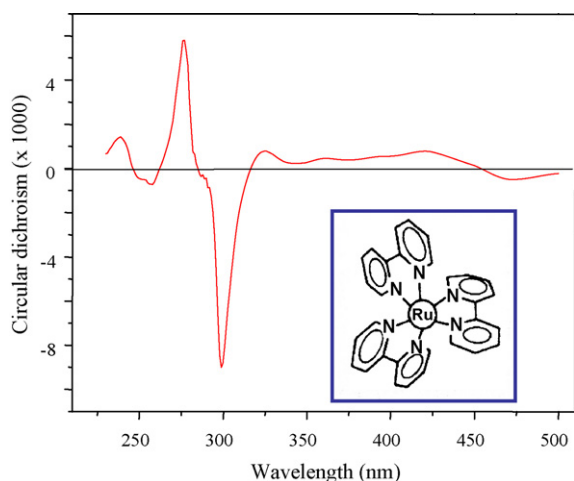


**Fig. 1.** Circular dichroism spectrum of enantiomerically pure  $\Delta$ -ruthenium tris(phenanthroline) in optical density units. The cell thickness is 1 mm and the concentration is 150  $\mu\text{M}$ . The inset shows the propeller shape of ruthenium tris(bipyridyl).

terized by two well-defined regions (Fig. 1): a strong bisignate structure around 280 nm assigned to the in-ligand transitions and a weaker one in the visible assigned to the MLCT transition. We have investigated these two spectral regions after excitation of the MLCT transition. Results are displayed in Fig. 2 (visible range, ruthenium tris(bipyridyl)) and Fig. 3 (UV range, ruthenium tris(phenanthroline)). In the visible region, most of the effects are connected to the bleaching of the MLCT transition [12]. This bleaching effect has also been observed in a one-beam experiment where a decrease of the CD with the light intensity was clearly observed [13]. This was the first experimental demonstration of an intensity-dependent CD as theoretically expected [14]. In that former study, we investigated nonlinear CD which is somewhat different of TRCD that we are considering in this article. Here, we are more interested in linear CD of excited molecules and its temporal

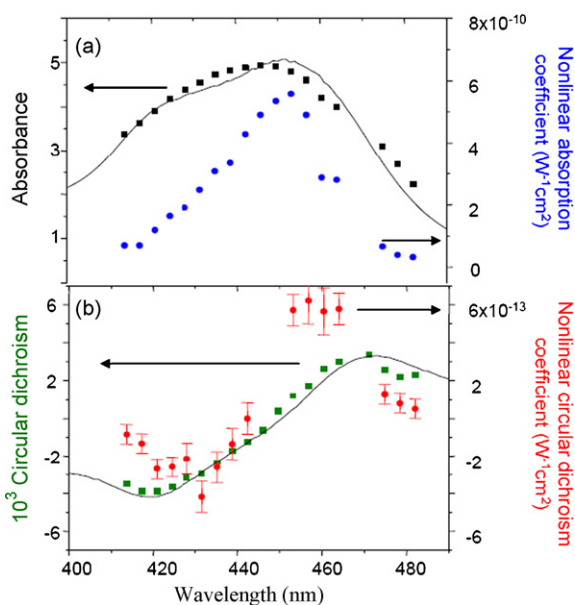


**Fig. 2.** Linear (squares) and nonlinear (dots) absorption (a) and CD (b) measured in a pump-probe experiment as a function of the probe wavelength in  $\Delta$ -ruthenium tris(bipyridyl). The pump wavelength is 465 nm and the pump-probe delay is kept fixed at 50 ps. The linear values are measured for a cell thickness of 2 mm. The nonlinear coefficients are given in absolute units ( $\text{W}^{-1}\text{cm}^2$ ) (see Ref. [12]). The solid lines are the spectra measured with commercial spectrophotometers.

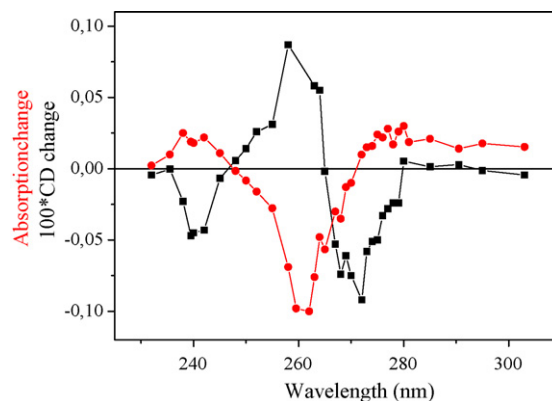


**Fig. 3.** Differential absorption (dots) and CD (squares) spectra of  $\Delta$ -ruthenium tris(phenanthroline) measured 50 ps after the excitation of the MLCT band. Absorption and CD are expressed in optical density (cell thickness = 1 mm).

evolution whereas nonlinear CD deals with the variation of CD with intensity. Interested reader can find details in [13]. Unfortunately, more precise interpretation of pump-induced CD in ruthenium tris(bipyridyl) in this spectral range is very uneasy because CD is due to complex coupling between the MLCT transition and higher-lying states [15]. Such is not the case in the UV region. In this region, the strong bisignate structure observed in the CD spectrum is the direct consequence of the coupling of the degenerate  $\pi$ - $\pi^*$  transitions taking place in the three ligands [16]. The simplicity of this origin has allowed us to carefully analyze the origin of the pump-induced CD. After excitation by the pump, an electron is promoted to one of the ligands and the ruthenium ion is now ligated to two *phen* ligands and to a *phen*<sup>-</sup> one, the transitions of which are known by excited-state absorption [17]. Thanks to a classical calculation of the coupling between these transitions, we have been able to model the CD spectrum of the MLCT state and identify its various components [18]. The results of the calculation are plotted in Fig. 4. The dotted curve corresponds to the ground-state CD whereas the solid curve corresponds to the MLCT CD. This last curve can be decomposed into two contributions: one coming from the unperturbed *phen* ligands and one coming from the *phen*<sup>-</sup> ligand. The CD of the unperturbed *phen* ligands can be understood within the degenerate coupled oscillator model. However, because only two oscillators are coupled, the energy shift as well as the rotational strengths are strongly reduced compared to the ground state case. Furthermore, the two rotational strengths are not perfectly opposite due to the

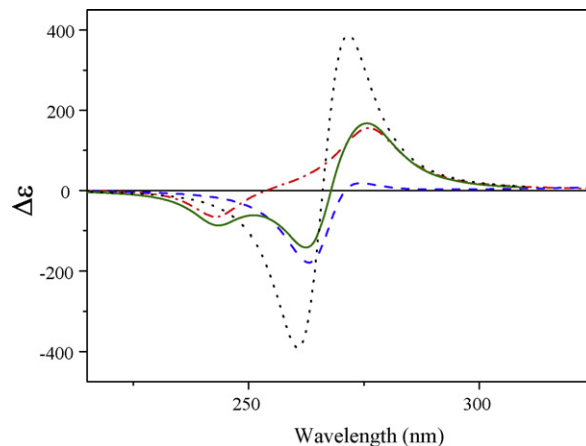


**Fig. 4.** Calculated CD spectra: (dotted line) ground state; (solid line) MLCT state. The MLCT spectrum can be decomposed into the unperturbed *phen* ligand contribution (dashed line) and in the *phen*<sup>-</sup> contribution (dot-dashed line).

influence of the other levels. On the contrary, the CD of the *phen*<sup>-</sup> ligand is closer to the non-degenerate coupled oscillator model. Its original three transitions experience almost no shift but a rotational strength appears for each, a negative one for the highest ( $\pi \rightarrow \pi^*$ ) transition and two positive ones for the lowest ( $\pi^* \rightarrow \pi^*$  and LMCT) ones. Note that the  $\pi^* \rightarrow \pi^*$  transition which takes place at 3.1 eV is not represented in Fig. 4. The total MLCT CD spectrum is the superposition of a bisignate CD structure due to the unperturbed ligand and of three monosignate ones due to the *phen*<sup>-</sup> ligand. Blue-shift of the  $\pi \rightarrow \pi^*$  transition in the reduced *phen*<sup>-</sup> ligand is responsible for the major change in the MLCT CD. By lifting the degeneracy of the three ligands, it profoundly modifies the coupling conditions and therefore strongly reduces the bisignate CD structure due to excitonic coupling.

It is worthwhile noting that we could not observe any dynamics on a 1.5 ns timescale. This result was expected for the pump-induced absorption since lifetimes of these compounds are in the hundreds of nanoseconds range. The absence of dynamics for the pump-induced CD shows that no change in the ligands positions or orientations occurs after the initial electronic excitation.

#### 4. Conformational dynamics in binaphthol

As mentioned earlier, the major interest of TRCD is to access information on the ultrafast dynamics of conformational changes occurring in photoexcited molecules. Such information is not easily accessed with usual pump-probe experiments where only the probe absorption is monitored because absorption is generally not very sensitive to conformational aspects. In this section, we present experiments that we have carried out on the ultrafast conformational relaxation occurring in (R)-(+)-1,1'-bi-2-naphthol (BINOL) after electronic excitation. BINOL is made up of two naphthol moieties linked by a C–C bond. The dihedral angle between the two moieties is about 104° in the ground state, at the origin of the chirality of this molecule [19]. Although it is well known that in such biaryl systems, the dihedral angle tends to decrease in the excited state [20], very few information exists on the dynamics of this process. Only a few experiments based on time-resolved absorption are available where information on the dihedral angle are obtained in an indirect manner [21,22]. We have therefore taken advantage of the intrinsic sensitivity of CD to investigate the dihedral angle dynamics in BINOL. The absorption and CD spectra are plotted in Fig. 5. We excite the BINOL molecule with a 267 nm pump pulse which provokes the electronic  $\pi \rightarrow \pi^*$  excitation in the naphthol moieties. Time-resolved absorption measurements do not reveal any dynamics on a 300 ps timescale, consistent with the known 5 ns lifetime of these excited states [23]. However, performing TRCD at 237 nm (corresponding to the bleaching of the <sup>1</sup>B<sub>b</sub> transition) and at 245 nm (corresponding to an excited-state absorption) brings quite different results, as depicted in Fig. 6 [24]. Examining the results obtained at 237 nm, one clearly sees that contrarily to what is observed in absorption, there is a relaxation process which takes place for the CD and that this relaxation is clearly solvent-dependent. For a very viscous solvent such as ethylene-glycol, no relaxation is observable whereas in ethanol this relaxation occurs in 100 ps. This feature can be confidently assigned to a relaxation of the dihedral angle in the excited state. The TRCD signal is the superposition of a ground state bleaching and of an excited-state one. A careful analysis of the TRCD curves [24] shows that the excited-state CD increases (in absolute value) with time, revealing that the dihedral angle decreases, a feature already inferred in binaphthyl from impulsive stimulated Raman measurements [25]. The two curves at 245 nm display the same increase of the CD in the excited-state absorption region when

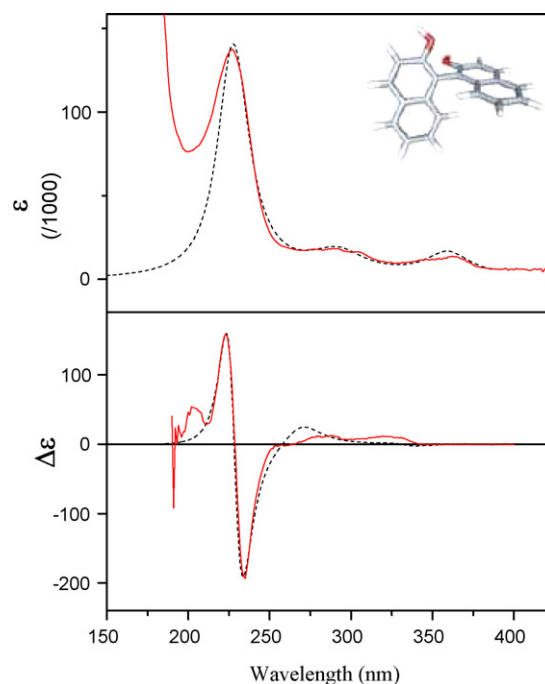


Fig. 5. Absorption and CD spectra of (R)-(+)-1,1'-bi-2-naphthol (in M<sup>-1</sup> cm<sup>-1</sup>; solid line). The dashed lines are fits obtained with the coupled oscillator calculation (see Ref. [24]). A sketch of the molecule is shown in the inset.

the dihedral angle decreases. An interesting information extracted from these two curves is that the relaxation time is much longer in a protic solvent compared to a nonprotic one, indicating that hydrogen bonding of the hydroxy groups in the naphthol moieties with the solvent play an important role for the dynamics of the dihedral angle. The 100 ps relaxation time measured in ethanol is compatible with the times measured by dielectric relaxation in this medium [26], explaining why the relaxation of the dihedral angle takes a much longer time for BINOL than for binaphthyl [21].

These experiments in BINOL bring a clear demonstration of the potentiality of TRCD to give information on the ultrafast dynamics of conformational changes.

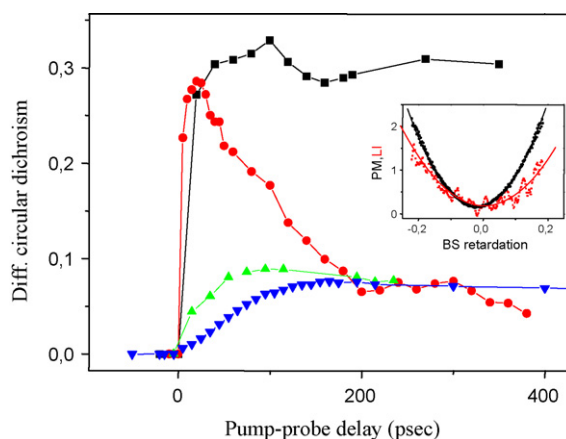
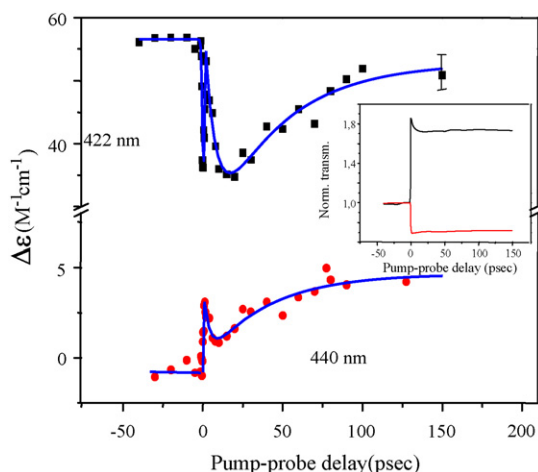


Fig. 6. Time-resolved CD in BINOL for two wavelengths and various solvents. Dots:  $\lambda = 237$  nm in ethanol; squares:  $\lambda = 237$  nm in ethylene-glycol; up triangles:  $\lambda = 245$  nm in cyclohexane; down triangles:  $\lambda = 245$  nm in ethanol. The inset shows the raw data: time-resolved CD is obtained by comparing the quadratic coefficients and the minimum positions for the PM and LI parabolas.





**Fig. 7.** Time-resolved CD following photodissociation of carboxy-myoglobin. Probe wavelengths are 422 nm (close to the MbCO absorption peak) and 440 nm (close to the Mb absorption peak). The two CD curves are fitted with two exponential functions (rise time = 7 ps, decay time = 43 ps). Inset: the corresponding normalized transmission curves.

## 5. Photodissociation of carboxy-myoglobin

Myoglobin is a 153 amino acid protein involved in the storage of oxygen in muscles. The heart of this protein is its cofactor, the heme, an iron-porphyrin capable of fixing ligands such as  $O_2$ , CO or NO. This protein has been extensively studied with time-resolved pump-probe techniques because when the heme is photoexcited, its central iron atom undergoes a low-to-high spin transition which provokes the detachment of the ligand. It is now well known that this photodetachment is accompanied by a doming of the heme which triggers conformational changes in the whole protein. In hemoglobin which consists of four sub-units similar to myoglobin, these conformational changes induce the passage from the relaxed form to the tense one which plays a dominant role in the allosteric effect. Photodissociation of carboxy-myoglobin is therefore a very attractive candidate for TRCD and we have carried out a whole set of experiments and calculations that we present now.

### 5.1. TRCD in the visible

Carboxy-myoglobin (MbCO) and deoxy-myoglobin (Mb) display a strong absorption feature taking place in the visible known as the Soret band. The position of the main peak depends on the spin state of the iron: it goes from 423 nm in MbCO to 434 nm in Mb. These strong absorption bands are accompanied by CD structures (cf. Fig. 9) and we have monitored the CD for these two peaks following photodissociation of the CO by a 400 nm pulse. On an electronic viewpoint, it is established that complete relaxation has occurred on a subpicosecond timescale [27] but that the heme has gone from the carboxy- to the deoxy ground state. Recombination of the CO takes place on a millisecond timescale and is therefore negligible in our measurements. Note that as expected, no dynamics is observable in the time-resolved absorption curves displayed in the inset of Fig. 7. On the other hand, we have observed a transient structure in the CD curves for the two wavelengths as displayed in Fig. 7. At negative delays, we recover the MbCO CD and in both case, a strong decrease of the CD occurs in about 10 ps, followed by a complete relaxation to the deoxy steady-state in 100 ps. This feature is at first sight surprising for two reasons: on the one hand, since the whole protein is involved in the conformational relaxation from the carboxy to the deoxy form, longer timescales are expected; on the other hand, the amplitude of the decrease of the CD signal is very strong. When looking on longer timescale, no further dynamics is

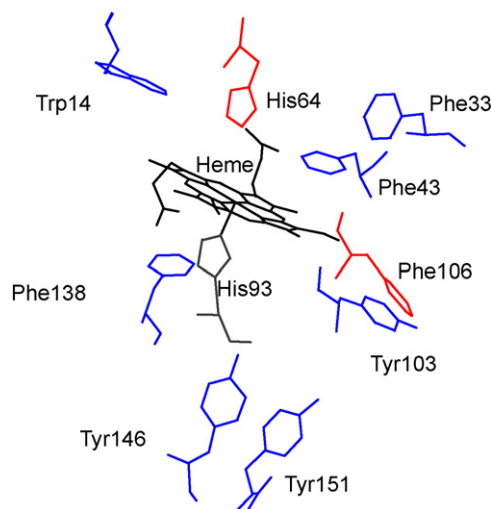


**Fig. 8.** Sketch of the main aromatic amino acids involved in the CD signal in the Soret band of MbCO (after PDB 1A6G).

observable. These observations show that what we measure cannot correspond to the mere passage from MbCO to Mb, but must involve some transient phenomenon. And because this feature is seen only in CD and not in absorption, we can expect this effect to be closely connected to some conformational change. In order to ascertain this point and to understand the origin of the transient CD signal, we have developed a classical CD calculation based on the coupled oscillator model.

### 5.2. CD calculation

Soret band CD in MbCO and Mb is known to occur from the coupling between the heme electronic transitions and those from the surrounding aromatic amino acids [28]. The change in conformation between steady-state MbCO and Mb is known from X-ray diffraction (Protein Data Bank 1A6G and 16AN for example). Configuration of the heme pocket from MbCO is depicted in Fig. 8. We have developed a calculation based on Applequist's coupled oscillator model. This calculation is detailed in Ref. [29]. The main results are summarized in Fig. 9. In this figure, the simulated CD spectra of various myoglobin species are plotted. The solid line is for MbCO

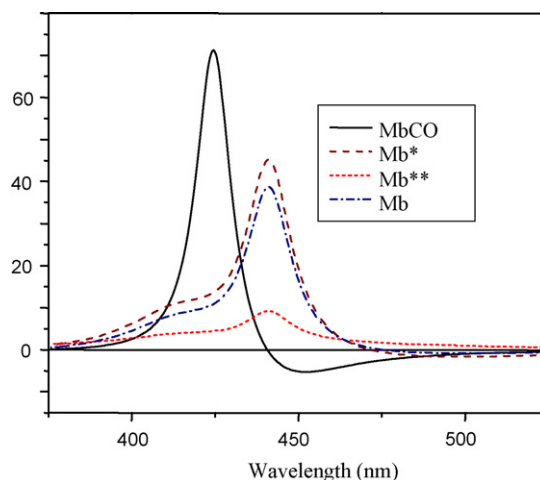


**Fig. 9.** Calculated CD spectra for MbCO (solid line) and Mb (long-dashed line) and for two intermediate configurations: MbCO conformation with the heme in its deoxy form (Mb\*) and same configuration with a 30° tilt of the proximal histidine (short-dashed line).

whereas the dot-dashed one is for Mb. They correspond to the starting and ending points in the photodissociation experiment. There is a large difference between these two curves, but it is clear that this difference primarily comes from the change in the electronic state of the heme when the iron goes from the low spin state to the high spin state. No conformational information can be extracted from these curves. In order to sort out the contribution in the TRCD curves coming from the change in the heme electronic state from possible conformational effects, we have modelled the CD spectrum of a fictitious protein where the conformation of the amino acids is the MbCO one whereas the heme electronic state is the Mb one. This corresponds to the dashed line (Mb\*). Surprisingly enough, this curve is very close from the Mb one, which means that the change in the protein conformation when going from the carboxy form to the deoxy one only translates in a very slight change of the CD. This slight change is not measurable and this feature explains why we do not observe any long-time dynamics in our TRCD curves even though conformational changes are still expected. The origin of the dip we observe in the TRCD experiments is therefore not understandable in terms of carboxy or deoxy form and one has to come up with other hypotheses. The main interest of our calculation is that it allows us to test many configurations by modifying the position of a unique amino acid for example. Out of a large number of trials, only one was able to provoke a strong decrease of the CD, when the proximal histidine was tilted (dotted curve in Fig. 9, Mb\*). Let us recall that the proximal histidine is the amino acid by which the heme is fixed to the F helix in the myoglobin backbone. Because it is the amino acid closest to the heme, it is strongly coupled to it and its tilting results in a dramatic decrease of the rotational strengths of the heme transitions [29]. This histidine tilting is only an artificial calculation effect, but it allows us to give an interpretation of our TRCD curves. When the CO gets detached from the heme, this latter undergoes a doming effect, which means that the iron atom goes below the heme plane. Because the proximal histidine is attached on one side the iron atom and on the other side to the F helix, this doming effect results in a squeezing of the histidine which is likely to provoke a deformation of the imidazole plane whose effect on the CD is similar to the tilt introduced in the calculation. This squeezing is then relaxed when the F helix is pushed towards its position in the deoxy protein. Our experiment therefore shows that this primary step in the passage from the carboxy to the deoxy form is finished in 100 ps. This time may seem very rapid since it involves the motion of many atoms, but it is in agreement with global energy relaxation times measured in myoglobin by Miller [30].

### 5.3. TRCD in the ultraviolet

As can be seen in the inset of Fig. 10, there are two spectral region in the UV where MbCO and Mb display a CD structure. The first one around 260 nm is likely to involve aromatic amino acids and especially tryptophan whereas the second one below 230 nm is known to correspond to the protein backbone. We have investigated TRCD in these two regions and results are depicted in Fig. 10. At 260 nm, we observe an instantaneous passage from MbCO to Mb. No dynamics is observable. This feature, in association with pump-induced absorption change measurements [5], is an indication that contrarily to what was expected, tryptophans do not play a dominant role in the CD signal in this region and here again, TRCD does not provide information on the long range motion involving the whole protein. On the other hand, the signal at 220 nm is very similar to the one observed in the visible with a rapid decrease followed by a total relaxation in 100 ps. Actually, the CD being negative at 220 nm (see inset), the TRCD corresponds to an increase in absolute value of the CD. This feature is quite interesting because it is well known that the CD at 220 nm is a signature of the presence of alpha helices in myoglobin. This transient increase of the CD can be tentatively

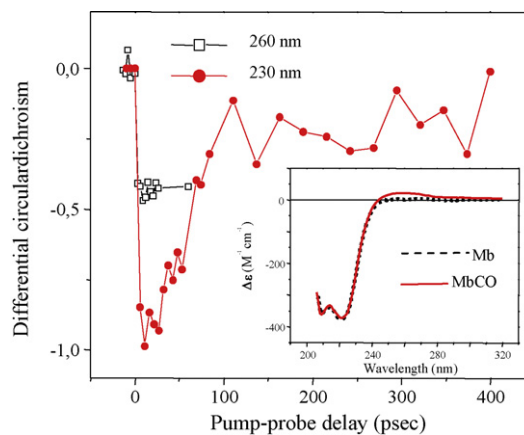


Fig. 10. Time-resolved CD (in arbitrary units) at 260 and 230 nm probe wavelengths following MbCO photolysis. Inset: steady-state CD spectra of MbCO and Mb in the UV.

assigned to a deformation of the F helix consecutive to the heme doming and to the aforementioned proximal histidine squeezing.

Visible and UV TRCD experiments are in agreement and thanks to the model calculation, their significance in terms of primary step in the transmission of the conformational changes from the heme doming to the protein relaxation can be confidently assigned. TRCD brings new information on the very first steps of the passage from the carboxy form to the deoxy one.

## 6. Conclusion and perspectives

This article has presented an overview of the work we have developed towards the implementation of TRCD techniques easily utilisable in ultrafast experiments. Several experiments have been presented which show the potentiality of TRCD to access new spectroscopic information or original conformational dynamics processes. In particular, the technical scheme based on the joint utilization of a Babinet–Soleil compensator on the probe and of a mechanical chopper on the pump is very promising since it provides a high sensitivity in a user-friendly experiment. We think that these techniques are now mature to investigate many relevant conformational processes taking place in molecules or biomolecules.

As already mentioned in Section 1, investigating rapid conformational changes in biomolecules is particularly appealing because many biochemical processes rely on the capacity of proteins to change their shapes and to modify or to adapt to their environment. Such is the case in most enzymatic reactions or in transmembrane signalling for example. Utilizing the chiroptical properties of proteins in time-resolved experiments is therefore a very promising way to access such information. Kligler's group has thoroughly developed this field by implementing not only TRCD [2] but also time-resolved optical rotatory dispersion [31] and applying these techniques to several proteins like myoglobin, [32] cytochrome c [33] or photoactive yellow protein [34] among others.

Among the issues most studied by biophysicists, protein folding is of paramount importance. The fundamental mechanisms at stake in the formation of globular protein are still strongly debated and much work is currently developed to decipher folding or unfolding processes in small peptides or proteins [35]. Up to now, the most direct probe of the secondary structure has been the amide I vibrational band lying in the infrared. This band is known to mainly arise from the C=O vibration in the peptide backbone and its position is very dependent on the secondary structure since these C=O bonds are strongly involved in the Hydrogen bonds which promote alpha helices or beta strands [36]. The main drawback of this spectroscopic probe is that it is by no way a quantitative one. Indeed, the

displacement of the amide I band when going from a  $\alpha$  helix structure to a random coil is about  $20\text{ cm}^{-1}$ , a small value compared to the total width of the amide I band ( $100\text{ cm}^{-1}$ ) which prevents a clear deconvolution of the various bands. Such is not the case for CD in the far-ultraviolet where the secondary structures give characteristic signatures. This feature is currently used to infer the proportion of secondary motives in an unknown protein. This is particularly true of the CD band lying at 220 nm which is in good approximation a direct signature of the presence of  $\alpha$  helices. However, CD being a very weak effect, its measurement cannot be carried out instantaneously and it is not possible to achieve a good time resolution by measuring directly the CD in a pump-probe set-up. Implementing the ultrafast techniques of TRCD described above in this wavelength range is therefore very promising.

We are currently developing such an experiment aiming at measuring TRCD at 220 nm in order to follow folding/unfolding of small peptides or proteins. In order to bring valuable information, TRCD experiments must be extended to longer time scales. The present pump-probe experiments where the pump-probe delay is provided by a variable optical delay line is limited to a few nanoseconds, a time much too short to apprehend complex phenomena such as protein folding. We are therefore developing a new pump-probe scheme based on the electronic synchronization of a nanosecond Nd:YAG laser and our Titanium-Sapphire system allowing delays between 10 ns and 1 ms to be accessed. Extending our TRCD detection system should not be an issue. The major problem, encountered by all the people working in this field is the optical triggering of the unfolding/folding process [37]. The simplest scheme is the T-jump where a nanosecond pulse is used to heat up water, provoking thermal unfolding of the peptides [38]. But other possibilities exist, such as pH-jumps [39] or photoswitchable peptides [40].

We think that TRCD will be an interesting alternative to other existing techniques which can bring complementary information and we hope that these techniques will develop in the near future.

### Acknowledgments

Hugues Mesnil, Thibault Dartigalongue and Claire Niezborala have performed most of the experimental work depicted in this article. Enantiomerically pure ruthenium complexes have been provided by the Laboratoire de Chimie de l'ENS-Lyon (Chantal Andraud's group).

### References

- [1] G.D.e. Fasman, Circular Dichroism and the Conformational Analysis of Biomolecules, Plenum Press, New York, 1996.
- [2] J.W. Lewis, R.F. Tilton, C.M. Einterz, S.J. Milder, I.D. Kuntz, D.S. Kliger, *J. Phys. Chem.* 89 (1985) 289.
- [3] X. Xie, J.D. Simon, *J. Am. Chem. Soc.* 112 (1990) 7802.
- [4] D.S. Kliger, J.W. Lewis, in: N. Berova, K. Nakanishi, R.W. Woody (Eds.), *Circular Dichroism—Principles and Applications*, Wiley-VCH, New York, 2000, p. 243.
- [5] T. Dartigalongue, C. Niezborala, F. Hache, *Phys. Chem. Chem. Phys.* 9 (2007) 1611.
- [6] T. Dartigalongue, F. Hache, *J. Opt. Soc. Am. B* 20 (2003) 1780.
- [7] C. Niezborala, F. Hache, *J. Opt. Soc. Am. B* 23 (2006) 2418.
- [8] V. Balzani, A. Juris, *Coord. Chem. Rev.* 211 (2001) 97.
- [9] P. Lincoln, B. Nordén, *J. Phys. Chem. B* 102 (1998) 9583.
- [10] R. Riesen, L. Wallace, E. Krausz, *Inorg. Chem.* 39 (2000) 5044.
- [11] J.R. Schoonover, K.M. Omberg, J.A. Moss, S. Bernhard, V.J. Malueg, W.H. Woodruff, T.J. Meyer, *Inorg. Chem.* 37 (1998) 2585.
- [12] H. Mesnil, M.-C. Schanne-Klein, F. Hache, M. Alexandre, G. Lemerrier, C. Andraud, *Phys. Rev. A* 66 (2002), 013802.1.
- [13] H. Mesnil, F. Hache, *Phys. Rev. Lett.* 85 (2000) 4257.
- [14] Y.P. Svirko, N.I. Zheludev, *Polarization of Light in Nonlinear Optics*, Wiley, Chichester, 1998.
- [15] P. Belsler, C. Daul, A. Von Zelewsky, *Chem. Phys. Lett.* 79 (1981) 596.
- [16] A. Rodger, B. Nordén, *Circular Dichroism and Linear Dichroism*, Oxford University Press, Oxford, 1997.
- [17] A. Hauser, E. Krausz, *Chem. Phys. Lett.* 138 (1987) 355.
- [18] C. Niezborala, F. Hache, *J. Phys. Chem. A* 111 (2007) 7732.
- [19] L. Di Bari, G. Pescitelli, P. Salvadori, *J. Am. Chem. Soc.* 121 (1999) 7998.
- [20] W. Rettig, M. Maus, in: J.E. Waluk (Ed.), *Conformational Analysis of Molecules in Excited States*, Wiley-VCH, New York, 2000, p. 1.
- [21] R.M. Bowman, K.B. Eisenthal, D.P. Millar, *J. Chem. Phys.* 89 (1988) 762.
- [22] D. Mank, M. Raytchev, S. Amthor, C. Lambert, T. Fiebig, *Chem. Phys. Lett.* 376 (2003) 201.
- [23] C.M. Harris, B.K. Selinger, *J. Phys. Chem.* 84 (1980) 891.
- [24] C. Niezborala, F. Hache, *J. Am. Chem. Soc.* 130 (2008) 12783.
- [25] S. Fujiyoshi, S. Takeuchi, T. Tahara, *J. Phys. Chem. A* 108 (2004) 5938.
- [26] J.T. Kindt, C.A. Schmuttenmaer, *J. Phys. Chem.* 100 (1996) 10373.
- [27] S. Franzen, L. Kiger, C. Poyart, J.-L. Martin, *Biophys. J.* 80 (2001) 2372.
- [28] M.C. Hsu, R.W. Woody, *J. Am. Chem. Soc.* 93 (1971) 3515.
- [29] T. Dartigalongue, F. Hache, *J. Chem. Phys.* 123 (2005) 184901.
- [30] R.J.D. Miller, *Annu. Rev. Phys. Chem.* 42 (1991) 581.
- [31] D.B. Shapiro, R.A. Goldbeck, D. Che, R.M. Esquerra, S.J. Paquette, D.S. Kliger, *Biophys. J.* 68 (1995) 326.
- [32] E.F. Chen, D.S. Kliger, *Inorg. Chim. Acta* 242 (1996) 149.
- [33] E.F. Chen, V. van Vranken, D.S. Kliger, *Biochemistry* 47 (2008) 5450.
- [34] E. Chen, T. Gensch, A.B. Gross, J. Hendriks, K.J. Hellingwerf, D.S. Kliger, *Biochemistry* 42 (2003) 2062.
- [35] S. Issue, *Chem. Rev.* 106 (2006) 1543.
- [36] W.K. Surewicz, H.H. Mantsch, D. Chapman, *Biochemistry* 32 (1993) 389.
- [37] M. Volk, *Eur. J. Org. Chem.* 2001 (2001) 2605.
- [38] R.H. Callender, R.B. Dyer, *Curr. Opin. Struct. Biol.* 12 (2002) 628.
- [39] S. Abbruzzetti, E. Crema, L. Masino, A. Vecli, C. Viappani, J.R. Small, L.J. Libertini, E.W. Small, *Biophys. J.* 78 (2000) 405.
- [40] H. Satzger, C. Root, C. Renner, R. Behrendt, J. Moroder, J. Wachtveitl, W. Zinth, *Chem. Phys. Lett.* 396 (2004) 191.